Crowding Effects on the Structural Transitions in a Flexible Helical Homopolymer

Alexander Kudlay,[1] Margaret S. Cheung,[2] and D. Thirumalai[1,3]

[1]*Biophysics Program, Institute for Physical Science and Technology, University of Maryland, College Park, Maryland 20742, USA*
[2]*Physics Department, University of Houston, Houston, Texas 77204, USA*
[3]*Department of Chemistry and Biochemistry, University of Maryland, College Park, Maryland 20742, USA*

(Received 4 January 2008; published 16 March 2009)

We elucidate the structural transitions in a helical off-lattice homopolymer induced by crowding agents, as a function of the number of monomers (N) and volume fraction (ϕ_c) of crowding particles. At $\phi_c = 0$, the homopolymer undergoes transitions from a random coil to a helix, helical hairpin **HH**, and helix bundle **HB** structures depending on N, and temperature. Crowding induces chain compaction that can promote **HH** or **HB** formation depending on ϕ_c. Typically, the helical content decreases which is reflected in the decrease in the transition temperatures that depend on ϕ_c, N, and the size of the crowding particles.

DOI: 10.1103/PhysRevLett.102.118101 PACS numbers: 87.15.A−, 87.14.E−, 87.15.Cc, 87.15.hp

The volume fraction (ϕ_c) of large macromolecules such as lipids, ribosome, and cytoskeleton fibers [1] in the cell interior, which can be as large as 0.4 [2], affects all biological processes ranging from transcription to folding of RNA and proteins. Protein stability [3,4] and folding rates [5] are enhanced by an entropic stabilization mechanism (ESM) according to which the predominant contribution to the native state stabilization is due to an increase in the free energy of the unfolded states. Entropy decrease of the unfolded states results from the suppression of the number of allowed conformations of the polypeptide chains due to volume excluded by the crowding particles, while the native state is affected to a lesser extent. The ESM [3,5] is linked to crowding agent-induced depletion attraction [5–8] between the monomers of the protein or RNA [9]. Crowding agents can also profoundly affect protein-protein interactions [10] and amyloid formation [11] that is linked to a number of neurodegenerative diseases.

Here, we consider crowding effects on the random coil (**RC**) to helix **H** transition. The interplay between the multitude of interactions between the crowding agents and proteins (V_{CP}) and the intraprotein forces (V_P) makes it difficult to predict the structural changes that occur in a protein when $\phi_c \neq 0$. We study the effect of spherical crowding agents on an off-lattice model of a homopolymer chain [12], which undergoes a coil to helix transition as temperature (T) is varied when $\phi_c = 0$. The major results, which were obtained for polymers with different N and ϕ_c using molecular simulations, are: (a) The phase diagram is determined by a balance between the strength, γ, of the dihedral angle potential that is related to the local stiffness and the parameter δ, which specifies the strength of the hydrophobic attraction between the nonbonded beads, i.e., ones that are separated by three or more covalent bonds. As δ is varied, the homopolymer undergoes a series of structural transitions from a **RC** to **H**, helical hairpin (**HH**), and helix bundle (**HB**) at low temperatures, depending on N. For a fixed ϕ_c, crowding particles whose radius (r_c) is commensurate with the size of the monomer (r_m) [7,13] [$\frac{r_m}{r_c} \approx (1)$], have the largest effect in stabilizing the collapsed structures. (b) The r_c and ϕ_c-dependent transition temperature, $T_S(r_c, \phi_c)$, from **RC** to predominantly **HH** or **HB** changes dramatically depending on r_c and ϕ_c. For a fixed ϕ_c, the most significant change in $T_S(r_c, \phi_c)$ (compared to $\phi_c = 0$) occurs when r_c is on the order of the size of the monomer. The values of $T_S(r_c, \phi_c)$ saturate, at all N, when r_c becomes large. At a fixed r_c, $T_S(r_c, \phi_c)$ decreases as ϕ_c increases.

The conformations of a homopolymer chain, with N connected beads [12], are specified by the vector $\{r_i\}$, $i = 1, 2., \ldots, N$. The potential energy of the chain is a sum of bond-stretch potential, bond-angle potential, interactions associated with the $(N-3)$ dihedral angle degrees of freedom (V_D), and nonbonded potential (V_N) that determines the extent of tertiary interactions. The energy functions V_D and V_N are $V_D = \sum_i \gamma\varepsilon\{[1 + \cos(\phi_i + \frac{2\pi}{3})] + (1 + \cos 3\phi_i)\}$ and $V_N = \sum_{i\neq j}\varepsilon[(\frac{2r_m}{r_{ij}})^{12} - 2\delta(\frac{2r_m}{r_{ij}})^6]$ where $\varepsilon(= 1$ kcal/mol) specifies the energy of interactions between nonbonded beads i and j separated by $r_{ij} = |r_i - r_j|$, γ ($= 1$ in this work) is the strength of the of the dihedral potential, ϕ_i is the ith dihedral angle, and $r_m = 2$ Å is the size of a monomer. The potential $V(= V_{CC} + V_{CP})$, arising from interactions between the spherical crowding particles (V_{CC}) and with the monomers (V_{CP}) is $V = \sum_{i\neq j}\varepsilon[(\frac{2r_c}{r_{ij}})^{12}] + \sum_{i,j}\varepsilon[(\frac{r_c + r_m}{r_{ij}^{CP}})^{12}]$ where r_{ij} is the distance between the crowding particles i and j, r_{ij}^{CP} is the distance between bead i and the crowding particle j, and r_c is size of the crowder.

The simulations were performed using a modified in-house AMBER6 [14] package that was altered to incorporate Langevin dynamics in the low friction limit [15] to enhance the rate of conformational sampling [16]. In the presence of crowders, the calculations were performed in

the NVT ensemble. The homopolymer and the crowding particles were confined to a cubic box and periodic boundary conditions are used to minimize surface effects. The size of the simulation box was determined by the condition that the box contain a minimum of 150 crowding particles. For small r_c, the edge of the box was equal to the sum of the length of the fully extended helix and four times the average distance between the crowders at a specified ϕ_c. The number of crowding particles ranged from ≈150 for the most dilute system with the largest r_c, to 1200 ($\phi_c = 0.2$, $r_c = 2$ Å, $N = 16$), and 3000 ($\phi_c = 0.2$, $r_c = 4$ Å, $N = 64$).

The sampling efficiency in the simulations were enhanced using the replica exchange method (REM) [5,17], which ensured that the thermodynamic averages are fully converged. We used 20 replicas in the temperature range from $T = 100$ to 400 K in the REM simulations. The initial configurations were randomly chosen from high-temperature simulations, and subsequently quenched to the desired temperatures. The integration time step was $10^{-4}\tau_L$ where $\tau_\tau = (mr_m^2/\varepsilon)^{1/2}$ with m being the mass of a bead. At chosen time interval ($= 40\tau_L$), configurations with neighboring temperatures were exchanged. The acceptance probability, which depends on the temperatures and the energies of the replicas, was in the range 0.2–0.3. In order to calculate averages, we retained between (4000–8000) conformations for each replica. The results of the REM simulations were combined with independent data set generated using the weighted histogram analysis method (WHAM) [18] to obtain thermodynamic averages. The structural transitions in the hompolymer were characterized by using the specific heat C_V and the radius of gyration R_g. The extent of helical order was quantified using $f_H(T, \phi_c) = \frac{1}{N-3}\sum_{i=1}^{N-3}\langle\Theta(\Delta\phi - |\phi_i - \phi_i^N|)\rangle$ where $\Theta(x)$ is the Heaviside function, ϕ_i^N is the value of the ith dihedral angle in the energy-minimized ($T = 0$) helical state, and $\Delta\phi$ is the tolerance in ϕ_i used to assign helical character to the ith dihedral angle. We chose $\Delta\phi = 12.07°$ to ensure that T_S obtained using the criterion $F_H(T_S, \phi_c = 0) = 0.5$ is consistent with the temperature at which C_V for $N = 64$ has a maximum.

The structural transitions as a function of T and δ for $N = 16$ with $\phi_c = 0$ [Fig. 1(a)] show that the **RC** → **H** transition occurs at $T_S \approx 292$ K at $\delta = 0$. For low to moderate δ values ($\delta \lesssim 0.5$), the polymer exists either as a **RC** or a **H**. With $\delta = 0.75$, we find a transition to a **HH** that is accompanied by a drastic reduction in R_g. At high δ values, the energy cost to form a bend in **HH** is compensated by a number of favorable tertiary contacts that stabilize the **HH**. The chain compaction at high δ results in structures that have high helical content as measured by $f_H(CT, \phi_c)$. For $N = 32$ and 64, besides **H** and **HH**s, we find that **HB**s can also form as δ and T are changed. For some range of δ, the ordered structures coexist, while for other choices, the probability distribution is peaked around

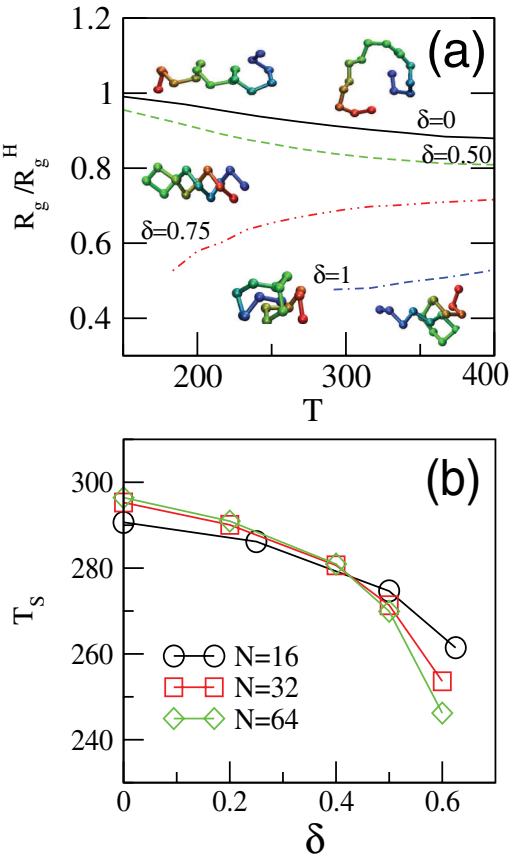

FIG. 1 (color online). (a) Normalized radius of gyration R_g/R_g^H as a function of temperature for several values of the short-range attraction parameter δ for the $N = 16$ chain. Snapshots of typical conformations are also shown. The value of $R_g^H = 10.1$ Å. (b) Transition temperature T_S as a function of δ for $N = 16$, 32, and 64.

only one unique structure. The transition temperature T_S at which the ordered structures form changes dramatically as δ increases [Fig. 1(b)]. Only when $\delta > 0.5$ do we find significant dependence of $T_S(\delta, \phi_c)$ on N [Fig. 1(b)].

From the temperature dependence of the thermally averaged R_g with $\phi_c = 0.2$ and at various sizes of r_c, we find that smaller crowding agents ($r_c = 2$ or 4 Å) are most efficient in inducing chain compaction [Fig. 2(a)]. For $r_c = 2$ Å, the values of R_g even at high temperatures are considerably smaller than R_g^H—the radius of gyration of the energy-minimized helical structure ($T = 0$). A qualitative explanation follows from the Asakura-Oosawa (AO) theory [7], which predicts that the strength of the additional entropically induced effective attraction between the beads increases as r_c decreases and ϕ_c increases. As a result, the effective attraction $\delta_R(\phi_c, r_c) \sim \delta_0 + f(\phi_c, r_c)$, which increases with decreasing r_c [19], is largest for small r_c. In the helical homopolymer model, a reduction in R_g, at sufficiently large δ, is also accompanied by enhancement in helical order which explains the emergence of

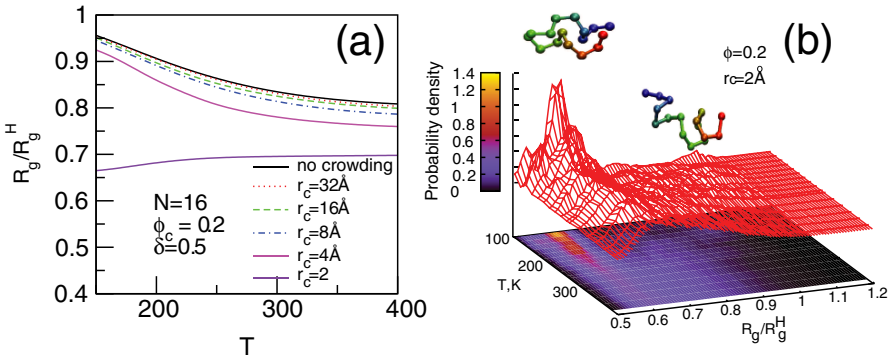

FIG. 2 (color online). (a) Normalized radius of gyration R_g/R_g^H as a function of T for different crowder radii r_c (indicated in the Figure) at $\phi_c = 0.2$ and $N = 16$. (b) Probability distribution functions of R_g/R_g^H for different temperatures for $\phi_c = 0.2$ and $r_c = 2$ Å case in (a).

HH [Fig. 2(b)]. Thus, crowding agents with $\frac{r_m}{r_c} \approx (1)$ are most efficient in inducing ordered structure formation at high T even if δ is not large.

The probability density, $P(T, R_g/R_g^H)$, in Fig. 2(b) for $\phi_c = 0.2$ shows that the distribution function changes continuously as T decreases. At high temperatures, there is one broad peak that represents an ensemble of mostly random coil **RC** structures. As T decreases below $T_S(r_c, \phi_c)$, a sharp peak that corresponds to **HH** structures, with high $f_H(T, \phi_c)$, emerges. Since there is only a continuous shift in $P(T, R_g/R_g^H)$, without a discernible region of bimodality, the transitions to structures with high $f_H(T, \phi_c)$ are not "phase transitions." Rather, the energy landscape has multiple basins of attraction with varying helical content whose population can be altered by changing T, ϕ_c, or δ.

Transitions to higher order (three or more) **HB** structures occur for $N = 64$ with $\phi_c = 0.2$ and $r_c = 4$ Å (Fig. 3). In this case, crowding-induced formation of **HH** and **HB** at low T is also accompanied by a dramatic reduction in R_g [Fig. 3(a)]. As temperature decreases, there is evidence for coexistence between long **HH** and **HB** [Fig. 3(b)]. The formation of a large number of interhelical contacts compensates for the energetic cost due to bend formation which results in the transition to the **HB**.

The volume fraction ϕ_c can be independently altered by changing either r_c or the number density of the crowding agents. For a fixed N and r_c, the values of $T_S(r_c, \phi_c)$ decrease as ϕ_c increases [Fig. 4(a)]. The variations are larger for the smaller r_c [Fig. 4(a)]. The decrease in $T_S(r_c, \phi_c)$ with increasing ϕ_c is a consequence of the enhancement in $\delta_R(\phi_c, r_c)$ caused by the entropic depletion attraction. From the AO theory, it follows that the strength of the depletion attraction $f(\phi_c, r_c)$ should increase as ϕ_c increases. Thus, $T_S(r_c, \phi_c)$ should have the largest shift as ϕ_c increases, which is in accord with our simulations [Fig. 4(a)].

The transition temperatures $T_S(r_c, \phi_c)$ [obtained using $f_H(T_S, \phi_c) = 0.5$] reports on the total helical content independent of whether the structure is an **H**, **HH** or **HB**. The changes in $T_S(r_c, \phi_c)$ for a fixed ϕ_c and varying r_c are shown in Fig. 4(a). We expect that as r_c increases beyond R_g^H the transition temperature $T_S(r_c, \phi_c)$ should approach the value expected for folding in narrow confined space formed by large crowding agents, and hence be independent of r_c. This is borne out by the simulations which show that $T_S(\phi_c, r_c)$ is almost constant as $r_c > 30$ Å [Fig. 4(b)]. For smaller values of r_c, Fig. 4(b) shows that T_S decreases sharply especially for $N = 16$. As in Fig. 4(a), we find that the largest changes are obtained for $r_c = 2$ Å.

The stability of helical conformations is determined by interplay of the local stiffness and the specific attractive interactions between beads i and $i + 3$. In contrast, crowding agents, which enhance nonspecific homogeneous attraction between the beads, induce chain compaction. Whether chain compaction is also accompanied by enhanced helical stability depends on the range and the strength of the AO attraction. At all values of r_c, the transition temperatures $T_S(r_c, \phi_c)$ decrease as r_c decreases with the change being most dramatic for small r_c

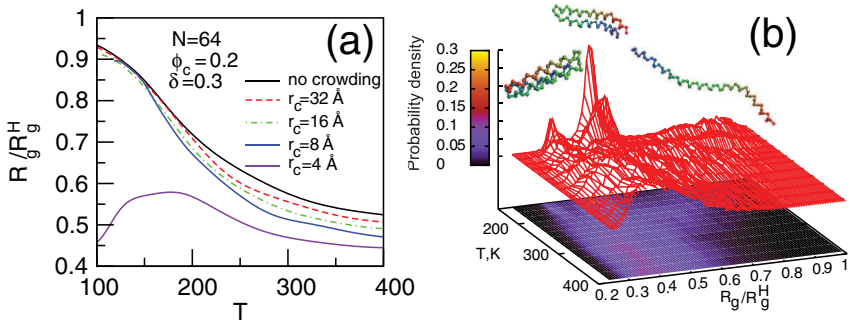

FIG. 3 (color online). Same as Fig. 2 except $N = 64$. (a) Normalized radius of gyration R_g/R_g^H (with $R_g^H = 40.4$ Å) at constant $\phi_c = 0.2$. (b) Probability distribution functions of R_g/R_g^H for the $\phi_c = 0.2$ and $r_c = 4$ Å case shown in (a).

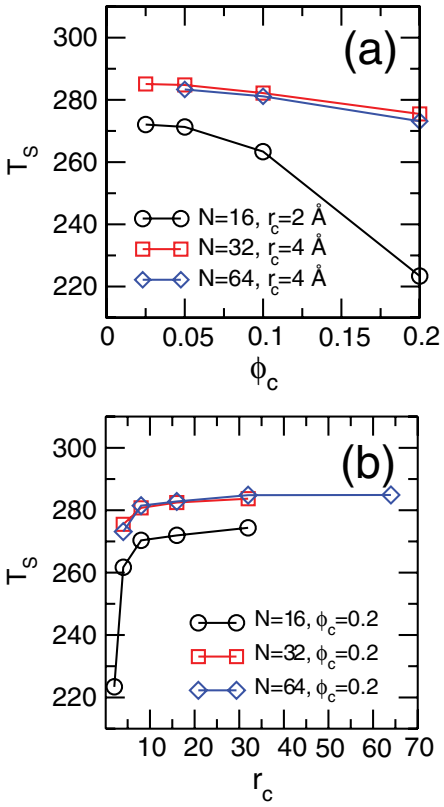

FIG. 4 (color online). (a) Helix-coil transition temperature $T_S(r_c, \phi_c)$ as a function of ϕ_c at a constant r_c for three chains with $N = 16$ ($r_c = 2$ Å), $N = 32$ ($r_c = 4$ Å), and $N = 64$ ($r_c = 4$ Å). (b) $T_S(r_c, \phi_c)$ as a function of the crowder radius r_c at $\phi_c = 0.2$. Plots for chains of lengths $N = 16$, 32, and 64 are shown. In both (a) and (b), $\delta = 0.3$.

[Fig. 4(b)]. These results show that the helical stability decreases when ϕ_c is nonzero even though the chain is compact. Thus, we conclude that the homogeneous AO attraction compromises the forces required to stabilize particular (**H**, **HH**, or **HB**) helical states. If the polymer backbone were stiff ($\gamma > 1$), then stretches of helical conformation on the scale of the persistence length of the chain would persist especially at low temperatures [8]. For the flexible helical polymer, there is a loss in helical stability, which is manifested by a decrease in $T_S(r_c, \phi_c)$ that is most pronounced when r_c is small.

We conclude with the following remarks. (1) Variation of the nonzero hydrophobicity parameter δ leads to a variety of higher order structures at low temperatures, such as **HH** and **HB**, whose stabilities can be enhanced by macro molecular crowding. (2) The high temperature denatured structures are more compact at $\phi_c \neq 0$ [see Figs. 2(a) and 3(a)] than when $\phi_c = 0$, which has implications for crowding-induced folding mechanisms of proteins. (3) Crowding-induced stabilization [20] can be rationalized using the ESM [5,21]. Our prediction that the helix stability changes, as ϕ_c and r_c are varied, can be validated using circular dichroism (CD) spectroscopy that detects the extent of helix formation in proteins [22].

We are grateful to E. O'Brien and N. Toan for useful discussions. This work was supported by a grant from the National Science Foundation through Grant No. CHE 05-14056. M. S. C. appreciates support from the University of Houston.

[1] O. Medalia, I. Weber, A. S. Frangakis, D. Nicastro, and W. Baumeister, Science **298**, 1209 (2002).
[2] R. J. Ellis and A. P. Minton, Nature (London) **425**, 27 (2003).
[3] A. P. Minton, Curr. Opin. Struct. Biol. **10**, 34 (2000).
[4] H. X. Zhou, Acc. Chem. Res. **37**, 123 (2004).
[5] M. S. Cheung, D. K. Klimov, and D. Thirumalai, Proc. Natl. Acad. Sci. U.S.A. **102**, 4753 (2005).
[6] M. S. Cheung and D. Thirumalai, J. Mol. Biol. **357**, 632 (2006).
[7] S. Asakura and F. Oosawa, J. Chem. Phys. **22**, 1255 (1954).
[8] Y. Snir and R. D. Kamien, Science **307**, 1067 (2005).
[9] D. L. Pincus, C. Hyeon, and D. Thirumalai, J. Am. Chem. Soc. **130**, 7364 (2008).
[10] R. Rivas, J. A. Fernandez, A. P. Minton, Proc. Natl. Acad. Sci. U.S.A. **98**, 3150 (2001); N. Kozer and G. Schreiber, J. Mol. Biol. **336**, 763 (2004); N. Kozer, Y. Y. Kuttner, G. Haran, and G. Schreiber, Biophys. J. **92**, 2139 (2007).
[11] D. M. Hatters, A. P. Minton, and G. J. Howlett, J. Biol. Chem. **277**, 7824 (2002).
[12] Z. Guo and D. Thirumalai, J. Mol. Biol. **263**, 323 (1996); D. K. Klimov, M. R. Betancourt, and D. Thirumalai Folding & Design **3**, 481 (1998).
[13] S. Asakura and F. Oosawa, J. Polym. Sci. **33**, 183 (1958).
[14] D. A. Case, D. A. Pearlman, J. W. Caldwell, T. E. Cheatham, W. S. Ross, C. L. Simmerling, T. A. Darden, K. M. Merz, R. V. Stanton, and A. L. Cheng *et al.*, *AMBER6* (University of California, San Francisco, 1999).
[15] D. K. Klimov and D. Thirumalai, Phys. Rev. Lett. **79**, 317 (1997).
[16] T. Veishans, D. K. Klimov, and D. Thiruamalai, Folding & Design **2**, 1 (1997).
[17] Y. Sugita and Y. Okamoto, Chem. Phys. Lett. **314**, 141 (1999).
[18] S. Kumar, D. Bouzida, R. Swendsen, P. A. Kollman, and J. M. Rosenberg, J. Comput. Chem. **13**, 1011 (1992); J. D. Chodera, W. C. Swope, J. W. Pitera, C. Seok, and K. A. Dill, J. Chem. Theory Comput. **3**, 26 (2007).
[19] M. R. Shaw and D. Thirumalai, Phys. Rev. A **44**, R4797 (1991).
[20] K. Sasahara, P. McPhie, and A. P. Minton, J. Mol. Biol. **326**, 1227 (2003).
[21] A. P. Minton, Biophys. J. **88**, 971 (2005).
[22] M. Perham and P. Wittung-Stafhede, FEBS Lett. **581**, 5065 (2007).